Quantum Electronics **47** (5) 431–437 (2017) ©2017 Kvantovaya Elektronika and Turpion Ltd

https://doi.org/10.1070/QEL16353

A vacuum gauge based on an ultracold gas

V.B. Makhalov, A.V. Turlapov

Abstract. **We report the design and application of a primary vacuum gauge based on an ultracold gas of atoms in an optical dipole trap. The pressure is calculated from the confinement time for atoms in the trap. The relationship between pressure and confinement time is established from the first principles owing to elimination of all channels introducing losses, except for knocking out an atom from the trap due to collisions with a residual gas particle. The method requires the knowledge of the gas chemical composition in the vacuum chamber, and, in the absence of this information, the systematic error is less than that of the ionisation sensor.**

Keywords: *pressure measurement, vacuum gauge, laser cooling of atoms, laser trapping of atoms, atomic–molecular interactions, van der Waals forces.*

1. Introduction

Laser cooling and trapping of atoms [1, 2] have found wide application in physics and related fields. In experiments with degenerate quantum gases of atoms, the effects that had been previously only the subject of theoretical discussion, such as Bose condensation [3] and Fermi pressure [4], were observed. In a gas of ultracold atoms excited to the Rydberg states, algorithms of quantum informatics can be implemented [5]. Precision spectroscopy of ultracold gases has become the basis for the development of the most accurate and stable frequency and time standards [6, 7]. The interference of de Broglie waves allows angular and linear accelerations to be measured with high accuracy, including the gravitational acceleration [8]. A primary vacuum gauge based on the gas of ultracold atoms was implemented in [9]. In this paper, we examine the physical principles on which the vacuum gauge is based and describe its experimental implementation.

The known primary vacuum gauges [10, 11] operate on the same principle as the Torricelli manometer [12]: the gas pressure is balanced by the pressure in a liquid column. The lowest pressure measurable by this method is 10^{-1} Pa. Before the appearance of work [9], smaller pressures could only be measured by the secondary vacuum gauges, in contrast to the primary ones that require calibration, since they measure the physical quantities that cannot be correlated with the pressure based on the first principles. The most sensitive secondary vacuum gauges – ionisation sensors with a hot cathode – allow the pressure measurements down to the lower limit of 5.4×10^{-12} Pa [13]. The cause of systematic errors in the ionisation sensors is that their readings are dependent on the gas composition [14] as well as electric and magnetic fields. The readings are also influenced by the uncontrolled evaporation from the electrodes [15], their aging and pollution. In addition, there is no possibility of sensor calibration in the entire measurement range.

The metrological pressure standards [16], necessary for the calibration of secondary vacuum gauges, allow one to obtain pressures down to the lower limit of 10^{-10} Pa [17]. The lowest pressures have been obtained during the continuous gas inlet into a known volume. The volume pressure is calculated on the basis of the inlet parameters. To ensure that actual pressure in the volume is close to the calculated one, the gas pressure must be much greater than that in the absence of the inlet. This requirement limits the capability of pressure standards from below. At the lowest pressures, the gas absorption on the walls and evaporation lead to the deviation of the distribution of molecules in velocities from the equilibrium Maxwellian distribution, to the violation of the pressure isotropy and to the deviation of the pressure from the calculated one.

Systematic errors of the secondary sensors and calibration means indicate the need for primary vacuum gauges for pressures of less than 10^{-1} Pa. The possible applications of such vacuum gauges include:

(i) direct pressure measurement devoid of the secondary vacuum gauge errors;

(ii) secondary vacuum gauge calibration;

(iii) testing the pressure standards and ensuring their operation at the pressures being lower than those currently attained; and

(iv) development of new pressure standards.

In the course of experiments with ultracold atomic gases, it has been repeatedly noted that the loss of atoms from the traps depends on the residual gas pressure in the vacuum chamber [18–23]. These observations open a way to the vacuum measurements based on ultracold atoms. The size of the cloud of trapped atoms ranges from a few microns to a few millimetres, which allows the development of a sensor for local pressure measurements. In experiments on laser trapping of atoms, the residual gas pressure should not exceed 10^{-5} Pa, which sets an upper limit for the method applicability. Until recently, it was not possible to design a primary vacuum gauge because of the large number of physical pro-

V.B. Makhalov Institute of Applied Physics, Russian Academy of Sciences, ul. Ul'yanova 46, 603950 Niznii Novgorod, Russia; e-mail: vasiliy.makhalov@appl.sci-nnov.ru;
A.V. Turlapov Institute of Applied Physics, Russian Academy of Sciences, ul. Ul'yanova 46, 603950 Niznii Novgorod, Russia; Lobachevsky State University of Nizhni Novgorod, prosp. Gagarina 23, 603950 Niznii Novgorod, Russia; e-mail: turlapov@appl.sci-nnov.ru

Received 9 March 2017
Kvantovaya Elektronika **47** (5) 431–437 (2017)
Translated by M.A. Monastyrskiy

cesses that generally affect the loss of atoms in the trap, and because of the absence of a model that would take all these processes into account.

Designing of a primary vacuum gauge described in this paper has become possible since all channel losses were eliminated, except for the one associated with the direct 'knock-out' of atoms from the trap as a result of their collision with atoms and molecules of the residual gas. Such an elimination of the undesirable channels turned out possible owing to the choice of a suitable atom (lithium-6) and the trap type: use was made of a shallow optical dipole trap formed at the focus of a mid-IR laser radiation beam [24] . In this system, the number of trapped atoms decreases with time t according to the exponential law $\propto e^{-t/\tau}$, while the pressure P is related to the lifetime τ of atoms in the trap as follows:

$$\tau P = \text{const}. \quad (1)$$

The constant τ is calculated on the basis of a small number of parameters, i.e. the vacuum chamber temperature, chemical composition of the gas in the chamber and van der Waals coefficients C_6 describing the interaction of trapped atoms with the residual gas particles. The vacuum gauge operation at pressures of $10^{-9}-10^{-6}$ Pa is demonstrated. In the case when the gas chemical composition is unknown, the measurement error is substantially less than that using the ionisation sensor. The developed vacuum gauge is sensitive to weakly ionised gases, such as helium. Due to the absence of electrodes, the vacuum gauge can be used wherever there is a heavy surface contamination, as for example, in lithography using extreme ultraviolet radiation [25] and molecular-beam epitaxy [26].

In Section 2, we analyse the physical mechanisms that lead to the losses of trapped atoms and, in their majority, serve as a source of errors in vacuum metrology. Section 3 discusses the ways of eliminating these errors and presents a theory that relates the pressure to the rate at which atoms leave the trap. The choice of lithium-6 is justified in Section 4. Section 5 presents data on the vacuum gauge operation and confirms the absence of major systematic errors. A comparison with the ionisation sensor readings is made in Section 6.

2. Losses of ultracold atoms from traps

Atoms can be held in magneto-optical [18, 19], magnetic [27] and optical dipole traps [21]. Below we consider the loss mechanisms for each of them. In the general case, the losses depend on a large number of parameters, some of which are poorly controlled. Even the shape of the population decline curve is generally unknown. Therefore, to implement reliable vacuum measurements, most loss channels must be excluded.

Measurements of the loss rate of atoms from a magneto-optical trap (MOT) were used in [23] for pressure measurements. The vacuum gauge from work [23] is a secondary one, since it requires calibration by an ionisation sensor. The smallest measured pressure was 3.3×10^{-8} Pa. The dependence of this value on the alignment of laser beams in the MOT was noted; besides, this dependence was different in different installations [23]. There are loss channels in the MOT that do not depend on the pressure and, thus, introduce a systematic error into the measurement. These are loss channels due to the collisions with a spin flip between atoms both in the ground [28–30] and the excited states [30]. Such losses set a lower limit of the pressure measured by this method. There are also several effects that complicate the dynamics of losses. For example, after a collision with a background gas particle, the atom may leave the trap or remain in it, depending on the magnitude of its initial energy and the trap depth [30, 31]. The depth and energy, in turn, depend on the number of trapped atoms and may vary significantly due to the misalignment of the MOT beams. An independent measurement of the MOT depth is difficult, as evidenced, for example, by the fact that the depth in [32] was calculated from the pressure and the loss rate. The readings both of the MOT-based vacuum gauge and the ionisation sensor depend on the residual gas composition and the interferences in the form of magnetic fields.

In contrast to the MOT, both for magnetic and optical dipole traps, the presence of atoms in them does not result in the perturbation of the trapping potential. This facilitates the modelling of losses and the establishment of their relationship with pressure. Nevertheless, the rate of losses due to collisions with the background gas particles still depends on the trap depth and the trapped-atom energy distribution, which can vary due to the losses, complicating their analysis. In both magnetic and dipole traps, the concentration of the trapped atoms can be greater than in the MOT, since there is no light pressure of atoms on each other. With increasing concentration, a new loss channel appears, namely three-particle inelastic collisions that lead to the exothermic formation of molecules.

There are several loss channels that are only inherent in magnetic traps. First, such traps do not confine the atoms whose magnetic moment is directed along the magnetic field, in the spin state with the lowest energy. The atoms that fall into these states due to magnetic dipole–dipole collisions are lost from the traps without the background gas influence. This effect most strongly manifests itself with increasing concentration of the trapped atoms [33]. Second, in the simplest (quadrupole) magnetic traps, there is a single-particle loss channel due to the Majorana spin flip near the magnetic field's zero [34, 35]. Third, a large rarefied cloud of relatively hot atoms can be formed around the main cloud when loading the magnetic trap from the MOT, or during the subsequent evaporative cooling. The interaction of this cloud with a denser and colder core also complicates the dynamics of losses [36].

The loss mechanisms that are only inherent in optical traps arise from the interaction of atoms with laser radiation. Scattering of photons leads to heating of atoms and to the losses of atoms after they have acquired a sufficient energy, and also to the transition of atoms to the ground states with a higher energy. Such atoms are lost after the spin flip due to a collision with another trapped atom. In addition, the fluctuations of power and direction of laser beam propagation lead to the parametric heating of the atoms [37].

3. Vacuum gauge theory and suppression of systematic errors

The use of a shallow optical dipole trap at a frequency far from the atomic resonance frequency makes it possible to exclude all the loss channels not related to collisions with residual gas particles. The dependence of losses on the energy of trapped atoms is also excluded. As a result of these simplifications, a decrease in the number of the trapped atoms becomes exponential, and the loss process itself can be calculated from the first principles (see below). In addition, it is shown below that the results of the method of vacuum metrol-

ogy under consideration are not disturbed by the main types of perturbations, such as the effects of electric and magnetic fields. The optical dipole trap produces a potential $U = -{}^1\!/_2 \boldsymbol{dE}$, where $\boldsymbol{E}$ is the oscillating electric field; $\boldsymbol{d} = 4\pi\varepsilon_0\alpha\boldsymbol{E}$ is the induced dipole moment; α is the atom polarisability; and ε_0 is the vacuum permittivity. Scattering of photons can be minimised in the case if the trap is used in the 'far-detuning' regime [38], i.e. at a wavelength λ of the trapping light, which is two or more times higher than the resonant one. In scattering of photons, the Rayleigh scattering predominates. At the trap centre, where the laser radiation intensity is I_0, the Rayleigh-scattered light frequency is [39]

$$\Gamma_{\mathrm{Ray}} = \frac{64\pi^4}{3}\frac{\alpha^2 I_0}{\hbar c\lambda^3}. \tag{2}$$

In each scattering event, the energy transferred to an atom is equal to the doubled recoil energy $E_{\mathrm{rec}} = (2\pi\hbar/\lambda)^2/(2m)$, where m is the atom mass. It is possible to estimate the time τ_{ph} needed for an atom to acquire the energy of the order of the trap depth $U_0 = 2\pi\alpha I_0/c$:

$$\tau_{\mathrm{ph}} \sim \frac{U_0}{2\Gamma_{\mathrm{Ray}}E_{\mathrm{rec}}} = \frac{3}{128\pi^5}\frac{m\lambda^5}{\alpha\hbar}. \tag{3}$$

The dependence λ^5 enables the heating rate to be arbitrary small.

The heating and losses associated with fluctuations of the power and propagation direction of the trap's laser beam [37] can be suppressed by using a laser with a sufficiently low level of such fluctuations. For example, a heating time of more than 2.3×10^4 s [40] is reached, which can be further increased by means of additional stabilisation and a reduction of the trap's elasticity coefficient, because the rate of losses decreases with decreasing this coefficient.

An optical dipole trap holds the atoms regardless of their spin. By trapping atoms at the lowest hyperfine level, it is possible to exclude collisions with a spin flip, which determine the lower limit of the pressure measured by the MOT [23], and lead to the losses from magnetic traps [33]. The only process populating the spin states with a higher energy is Raman scattering. Herewith, for alkali metals and hydrogen, the scattered light frequency can be expressed through Γ_{Ray} [38]:

$$\Gamma_{\mathrm{Ram}} = \Gamma_{\mathrm{Ray}}\frac{8}{9}\left(\frac{\Delta\lambda_{\mathrm{fs}}}{\lambda}\right)^2, \tag{4}$$

where $\Delta\lambda_{\mathrm{fs}}$ is the wavelength difference corresponding to the fine splitting of the excited level with the largest oscillator strength. After excitation, the atom experiences an inelastic collision with another atom, which may result in a loss of both atoms from the trap. Thus, $2\Gamma_{\mathrm{Ram}}$ is the upper bound for the loss frequency due to Raman scattering. Such losses are suppressed by increasing λ and using an atom with a small value of $\Delta\lambda_{\mathrm{fs}}$.

Elastic collisions between the trapped atoms may lead to evaporation of the 'hottest' atoms from the trap [41]. Evaporative losses are usually small. Moreover, they can be completely eliminated by using a gas with a zero s-wave scattering length, such as fermions in the same spin state. Thus, it is possible to completely eliminate the collisional losses not related to collisions with the background gas.

The collision of a trapped atom with a background gas particle can have two outcomes: the atom leaves the trap and the atom remains in it, but with a greater energy. The latter outcome is undesirable, because it complicates the dynamics of losses by making it dependent on the energy distribution of atoms. Let us show that this undesirable outcome is excluded in a shallow trap. For an atom to stay in the trap, the angle θ of its scattering, as a result of the collision, should not exceed a small value $\theta_0 = \sqrt{2mU_0}/\mu v$ [42], where $\mu = mM/(m+M)$ is the reduced mass; and M and v are the mass and velocity of the incident particle, respectively. The scattering amplitude does not depend on θ in the regime of quantum diffraction at sufficiently small angles $\theta < \theta_{\mathrm{d}} = \lambda_{\mathrm{dB}}/(\pi r_0)$ [42], where λ_{dB} is the de-Broglie wavelength; and r_0 is the spatial scale of the interaction potential, which is related also to the total scattering cross section $\sigma \simeq 2\pi r_0^2$. Using the independence of the scattering amplitude on θ, we can calculate that the probability for an atom to be trapped is less than $\theta_0^2/\theta_{\mathrm{d}}^2 = U_0/E_{\mathrm{d}}$, where $E_{\mathrm{d}} \equiv 2\hbar^2/(mr_0^2)$ is the characteristic energy associated with the spatial scale r_0. Thus, at a sufficiently small ratio U_0/E_{d}, the atom is lost from the trap with a probability arbitrarily close to unity. Because of this, the loss cross section is equal to the collision cross section, which can be expressed through the van der Waals coefficient C_6 by the Landau–Lifshitz–Schiff formula [43]:

$$\sigma = 8.08\left(\frac{C_6}{\hbar v}\right)^{2/5}. \tag{5}$$

The flying away atom does not interact with the remaining atoms. For example, for a lithium atom moving with a velocity $v = 500$ m s^{-1}, the mean free path in a cloud with a concentration of 10^{10} cm^{-3} is $\sim$10 m.

Since only single-particle losses remain, the population decreases exponentially. The inverse lifetime of an atom in the trap is

$$\frac{1}{\tau} = n\langle v\sigma\rangle_T, \tag{6}$$

where n and T are, respectively, the concentration and temperature of the gas whose pressure P is measured; and $\langle\ldots\rangle_T$ is the averaging over the Maxwell distribution. As a result, the pressure $P = nk_{\mathrm{B}}T$ is related to τ as follows:

$$\tau P = 0.096\hbar^{2/5}(k_{\mathrm{B}}T)^{7/10}\frac{M^{3/10}}{C_6^{2/5}}, \tag{7}$$

where k_{B} is the Boltzmann constant. This is the basic formula of a vacuum gauge.

Table 1 gives the coefficients C_6 for the interaction of molecules of frequently used gases with lithium atoms [44]. The chemical composition of the gas in the chamber is assumed to be known. The constant in the right-hand side of (7) must be averaged over all gases:

$$\tau P = 0.096\hbar^{2/5}(k_{\mathrm{B}}T)^{7/10}\left(\sum_i \eta_i\frac{C_{6,i}^{2/5}}{M_i^{3/10}}\right)^{-1}, \tag{8}$$

where the subscript i indicates the parameters related to the ith gas, including its fraction η_i in the total concentration. The method can also be used in the case of an unknown chemical composition of the gas. In this case, an uncertainty in finding P arises, the value of which can be found according to the values of $M^{3/10}/C_6^{2/5}$ from Table 1. For the gases He, H_2, N_2 that are frequently used in vacuum technology, the constants

Table 1. The values of the coefficients C_6 and $M^{3/10}/C_6^{2/5}$ for the interaction of lithium atoms with molecules of the frequently used gases, and also the correction factors for the Varian UHV-24 ionisation sensor for the same gases.

Gas	C_6 (a.u.)	$M^{3/10}/C_6^{2/5}$ (a.u.)	Correction factor
H_2	83	2.0	0.46
He	22	4.2	0.18
N_2	180	3.2	1.0
Ar	180	3.6	1.3

Note: The atomic unit $C_6 = e^2 a_0^5/(4\pi\varepsilon_0)$, where a_0 is the Bohr radius; the atomic unit $M^{3/10}/C_6^{2/5} = m_e^{3/10}(4\pi\varepsilon_0)^{2/5}/(e^{4/5}a_0^2)$, where m_e and e are the mass and charge of the electron.

in the right-hand side of (7) differ no more than by a factor of 2.1, which limits the systematic error from above.

The error arising from the chemical composition uncertainty is, in most cases, less than that of an ionisation sensor with a hot cathode. In such sensors, the proportionality coefficient between the current and pressure is determined not only by the gas type, but also by the sensor design, since the ionisation probability depends on the velocity of electrons [15, 45]. Furthermore, there are no generally accepted data for the sensor's relative sensitivity to various gases (correction factors) [45–47]. As shown in work [14], the current in the helium atmosphere constitutes 0.12–0.18 of the current in nitrogen at the same pressure. At the same time, in the instruction manual for the Varian UHV-24 sensor (see Section 6), a correction factor of 0.18 is proposed.

4. Justification of the choice of lithium-6

Laser trapping and cooling have been successfully used for atoms of alkali metals (Li, Na, K, Rb, Cs, Fr), noble gases in metastable states (He, Ne, Ar, Kr, Xe), lanthanides (Eu, Dy, Ho, Er, Tm, Yb), elements of the 2nd group (Mg, Ca, Sr, Ba, Cd, Hg), chromium and silver. Laser cooling of alkali metals, with the exception of francium, is much simpler than that of other elements.

Among alkali metals, lithium has the lowest saturated vapour pressure at room temperature, which constitutes 10^{-18} Pa. This allows one to satisfy an important requirement: the presence of the vacuum gauge sensor should not perturb the pressure being measured. The vapour pressures of other alkali metals are as follows: 4×10^{-9} Pa (Na), 3×10^{-6} Pa (K), 3×10^{-5} Pa (Rb) and 2×10^{-4} Pa (Cs). Such high pressures impede the use of these alkali metals in vacuum measurements.

To gain the best sensitivity to low pressures, an atom with the highest C_6 values or, what is almost equivalent, with the highest static polarisability α, is needed. Caesium possesses the highest polarisability among alkaline metals. The C_6 coefficient for caesium is twice that for lithium, regardless of the residual gas composition. However, according to (7), the use of caesium instead of lithium increases the sensitivity only by a factor of 1.3. Thus, the sensitivity of a vacuum gauge utilising lithium is merely slightly less than that on other atoms.

The sensitivity spread of the vacuum gauge in relation to other gases cannot be reduced by replacing lithium with another alkali metal, since for all of them the parameter $M^{3/10}/C_6^{2/5}$ varies approximately in the same range as for lithium.

Due to a low mass, small values of U_0/E_d are easily attainable for lithium. This is important for exclusion of those collisions with the background gas, after which the atom remains trapped.

A small fine splitting of the levels in the lithium atom helps to get rid of the losses that result from the Raman scattering. For lithium, $\Delta\lambda_{fs} = 0.015$ nm, while for caesium $\Delta\lambda_{fs} = 42$ nm.

The fermion isotope ^{6}Li is particularly attractive for use in a vacuum gauge because of the ease of eliminating the losses associated with collisions between the trapped atoms. The atoms at the $2S_{1/2}(F = 1/2)$ level, in contrast to the atoms at the $2S_{1/2}(F = 3/2)$ level, do not experience inelastic two-particle collisions, since this level has the lowest energy. The centrifugal barrier for p-wave collisions is 7 mK [48], which leads to an exponential suppression of all partial scattering waves, except for s-waves, at the temperatures below 1 mK that are easily achievable in the process of laser cooling. In a zero magnetic field, the s-wave scattering length for fermions in the states with $m_F = \pm1/2$ is extremely small (much less than one Bohr radius [49]), which at $T = 100$ μK and the concentration of 10^{10} cm^{-3} gives a collision frequency much lower than 10^{-3} s^{-1}. At temperatures much smaller than U_0/k_B, a flow to the large-momentum states that are not captured in the trap is additionally suppressed by the exponentially small Boltzmann factor. Thus, in the ultracold gas ^{6}Li, the evaporative losses are zeroed without polarisation of fermions into a single magnetic state.

The above arguments indicate that ^{6}Li atoms are the best element for designing a vacuum gauge.

5. Experimental testing of the vacuum gauge

The vacuum gauge was experimentally tested on the setup presented in [50]. The vacuum chamber and key elements are shown in Fig. 1. During the measurement, vacuum in the chamber is provided by an ion pump with a nominal pumping rate of 75 L s^{-1} for nitrogen and a layer of titanium getter covering all surfaces, from which the filaments for titanium sputtering are visible. The noble gases have been removed beforehand by a turbo-molecular pump (during the experiment it was turned off). Before the experiment, the vacuum chamber was heated to 200 °C, while, during the experiment, the temperature in the chamber was kept at the room temperature.

An optical dipole trap is formed in the focus of a laser beam with a wavelength of $\lambda = 10.6$ μm and a Gaussian transverse mode. This wavelength significantly exceeds the wavelengths of electro-dipole transitions in ^{6}Li, the strongest of which has a wavelength of 671 nm. In the static-field approximation, the polarisability is $\alpha = 24.3\times10^{-30}$ m^3 [51]. A beam of laser radiation with a power of 60 W is focused into a spot with a radius of 44 μm at the intensity level of 1/e, while the Rayleigh length is 1140 μm, which gives the potential U_0 with a depth of 5.1×10^{-27} J (370 μK). The trap is not perturbed by homogeneous electric and magnetic fields. Strong gradients of the magnetic field or the electric field square can knock atoms out of the trap. In the direction orthogonal to the laser beam axis, this requires the gradients of $\sim$10 T m^{-1} and $\sim10^{17}$ V^2 m^{-3}, while the gradients being 20 times smaller are sufficient along the beam axis. Even smaller gradients of static fields disturb the trap shape, but do not affect the measurement results. The photon heating time $\tau_{ph} = 4\times10^7$ s does not depend on the trap depth, which

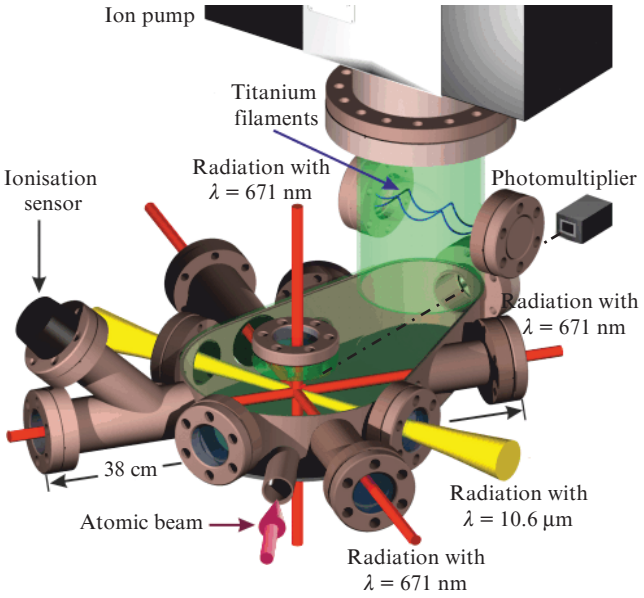

Figure 1. Vacuum chamber and key elements of the experimental setup. The direction to the photomultiplier is shown by a dot-and-dash line.

allows one to neglect the heating. The loss frequency due to Raman scattering $2\Gamma_{\mathrm{Ram}} = 10^{-15}$ s^{-1} is also negligible. For a collision of lithium with molecular nitrogen, the ratio U_0/E_{d} is equal to 0.002, and for a collision with He and H_2 the value of U_0/E_{d} is even smaller. Thus, the collisions with a background gas virtually always lead to the removal of the atom from the trap.

To measure the pressure, the atoms of ^{6}Li are loaded into the MOT from the atomic beam (Fig. 1). The beam is formed by a furnace at a temperature of 385 °C, inside which the lithium pressure is 0.01 Pa. The furnace is connected to the main vacuum chamber by a thin tube about 1 m long with differential pumping so that the pressure in the furnace does not affect the pressure in the chamber. Atoms in the beam are slowed down to a velocity of ~30 m s^{-1} by means of a Zeeman slower (not shown in Fig. 1). In the course of loading that lasts 7 s, 3×10^8 atoms are accumulated in the MOT, the cloud sizes are 1 mm vertically and 2 mm horizontally. The ^{6}Li vapour temperature in the MOT amounts to several hundred μK. During the MOT loading, the optical dipole trap is enabled; the centres of the two traps coincide. The MOT loading terminates with shutting down the laser beam of the Zeeman slower, whereas the atomic beam remains switched on throughout the entire experiment. Immediately after the loading, the MOT laser beams emptying the lithium level $2S_{1/2}(F = 1/2)$ are switched off, while the main MOT beams are switched off after 150 μs. This leads to the population transfer to the $2S_{1/2}(F = 1/2)$ level and to the formation of a comparable population of states with $m_F = \pm1/2$. After that, the MOT magnetic field is switched off, so that only the trapping power of the optical dipole trap remains. To ensure that the largest number of atoms is transferred from the MOT, the dipole trap during the MOT loading is initially formed by two counterpropagating beams and has a depth of $4U_0$. After switching off the MOT, one of these two laser beams is slowly 'quenched' within 0.6 s. About 5×10^5 atoms remain in a single beam in a trap with a depth of U_0. Then, the trap depth is gradually decreased threefold in 0.5 s, and after that it is smoothly restored for the same time. As a result, the gas fills the trap by no more than $1/\sqrt{3}$ of the depth U_0. This completes the ultracold gas preparation. The resulting cloud in the trap has a spindle shape with the size of $80\times80\times2000$ μm.

If the vacuum gauge theory (Section 3) is correct, the number of atoms in the optical dipole trap should decrease exponentially with time. The dependence of the number N of trapped atoms on the confinement time t was measured (Fig. 2). To perform such a measurement at the time moment t counted from the moment when the trap is filled, the cloud is illuminated by a beam of monochromatic radiation with a resonant wavelength of 671 nm. The fluorescence intensity, which is proportional to N, is measured by a photomultiplier (Fig. 1). The measurement destroys the cloud, and, to repeat the measurement, the experiment is performed anew, from the beginning of the loading of atoms into the MOT. To obtain the dependence in Fig. 2, fluorescence was recorded at the time moment t, and also five to six measurements were performed at $t = 0$. Next, the signal having been measured at the time moment t was divided by the average value of the signals at $t = 0$. In total, as many as 23 groups of such measurements were conducted, which took two hours. The standard deviation of the results in a single measurement at $t = 0$ constitutes 9%. Each error interval in the dependence presented in Fig. 2 is the standard error of the mean value for the groups of measurements performed at the corresponding time t. The error at $t = 0$ is absent due to the accepted procedure of data processing.

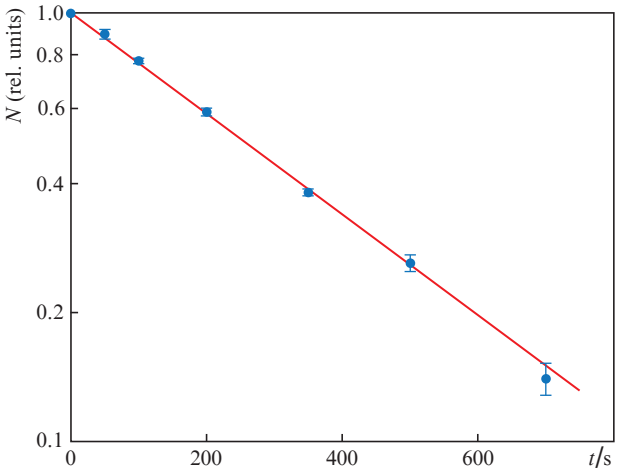

Figure 2. Number N of trapped atoms as a function of the confinement time t. The points are experimental data; the solid line is a result of approximation by the function $e^{-t/\tau}$.

Approximating the experimental data in Fig. 2 with the exponent $N(t) \propto e^{-t/\tau}$, we can find the time τ that constitutes 370 ± 6 s. It can be seen that the population decay is indeed exponential. In principle, to find τ requires the measurements only at two values of t.

The data in Fig. 2 have been obtained at the lowest pressure achieved in the stainless steel vacuum chamber at room temperature. The chemical composition of the gas in the chamber is unknown, and for its determination we use the data of authors of Refs [52–54]. They point out that, in stainless steel chambers under conditions of ultrahigh vacuum, the molecular hydrogen concentration is many times greater than that of the remaining gases. Assuming that only hydrogen

molecules are present in the chamber, we can find the pressure from formula (7):

$$P = 2.8\times10^{-9}\ \text{Pa}. \quad (9)$$

In this case, the main systematic error in determining P is related to the uncertainty of C_6 for Li–H_2 collisions, which amounts to 10% [44] and, as a result, yields an error of 4% for the factor $M^{3/10}/C_6^{2/5}$ and pressure. The error magnitude can be reduced by a more accurate calculation of C_6 using the methods described in [55–57]. The statistical error in determining P is equal to that in determining τ, the standard deviation being 1.6%.

The shape of the measured dependence $N(t)$ can be used for a critical evaluation of the method. First, this dependence does not contain the signs of losses associated with the heating of the gas by any mechanism. Since atoms initially only fill the trap to a depth of $(1/\sqrt{3})U_0$, heating, if any, should result in the loss of atoms from the trap only after some time delay required to increase the energy of atoms to the level of U_0. Second, if the atomic beam is cut off after the MOT loading is completed, the confinement time τ remains the same. This means that the atomic beam, whose trajectory passes at a distance of 15 mm below the dipole trap, does not knock out the atoms. Third, the exponential dependence $N(t)$ in Fig. 2 shows that all processes are of single-particle nature. Consequently, the dependence of losses on the number or concentration of atoms is excluded.

6. Comparison of the experimental results with the results of measurements using an ionisation sensor

The pressure determined from the lifetime of atoms in the trap ($P \equiv P_{\text{trap}}$) can be compared with the readings of the Varian UHV-24 ionisation sensor (P_{ion}) with a hot cathode. The sensor position is shown in Fig. 1. The lower limit of the sensor sensitivity is nominally 7×10^{-9} Pa (for nitrogen). At lowest pressures achieved in our setup, the ionisation sensor does not work. The pressure should be increased to fall into the sensitivity region of this sensor. For this purpose, the vacuum chamber region located near the lock for titanium filaments is locally heated. The highest pressure is attained at 140°C. For each pressure, the confinement time τ and the nominal (nitrogen) pressure recorded by the ionisation sensor are measured. To transform these two quantities into the corresponding P_{trap} and P_{ion} pressures, it is necessary to know the gas composition in the vacuum chamber. As known from the literature, in stainless steel chambers at a temperature up to 150°C, molecular hydrogen concentration greatly exceeds the concentration of other gases [52]. Therefore, we accept that H_2 is the only gas. The correction factor for conversion of the ionisation sensor readings from nitrogen to hydrogen is given in Table 1. The resulting data for comparison of the two measurement methods are shown in Fig. 3.

The gas temperature affects the measurement results obtained by both methods. When calculating P_{trap} and P_{ion}, room temperature was used, since the atoms coming from the heated region, both to the trap and the sensor, experienced repeated collisions with the vacuum chamber parts that were held at room temperature.

The pressure, determined from the loss rate of atoms from the trap, is 1.7 times greater than that measured by the ionisation sensor. Their values lie near the straight line $P_{\text{trap}} \propto P_{\text{ion}}$ passing through the coordinate origin. This is consistent with the assumption that the gas composition does not change when heated. The closeness of these data to the straight line also indicates that the pressures in the sensor region and in the trap vicinity are the same. Indeed, if the contribution to the pressure were introduced by any unaccounted sources, their relative contribution would decrease with increasing pressure. This would shift the data to the straight line $P_{\text{trap}} = P_{\text{ion}}$, which does not occur.

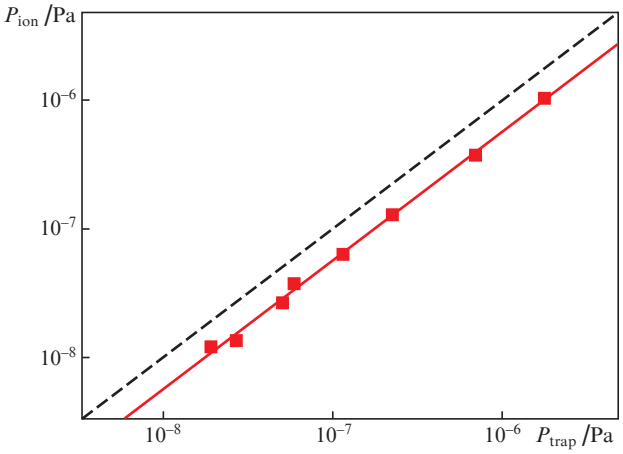

Figure 3. Comparison of the pressures measured according to the lifetime of atoms in the trap (abscissa axis) and by ionisation sensor (ordinate axis). The points are the experimental data, the solid line is the approximation of data by the $P_{\text{trap}} \propto P_{\text{ion}}$ dependence, the dashed line is $P_{\text{trap}} = P_{\text{ion}}$.

Thus, we have examined the use of an ultracold gas of atoms in a shallow optical dipole trap as a basis for the design of a primary vacuum gauge. The lifetime of the atom in a trap is related to the pressure by a linear formula whose only parameter is determined by the chemical composition of the gas and the van der Waals coefficients C_6. It is shown that the gas of lithium-6 is the optimal working body for such a vacuum gauge.

Acknowledgements. The authors are grateful to the Presidium of the Russian Academy of Sciences for the financial support (Fundamental Problems of Nonlinear Dynamics in Mathematical and Physical Sciences Programme). The work was also supported by the Russian Foundation for Basic Research (Grant Nos 14-22-02080-ofi-m, 15-02-08464, 15-42-02638).

References

1. Balykin V.I., Minogin V.G., Letokhov V.S. *Rep. Progr. Phys.*, **63**, 1429 (2000).
2. Onofrio R. *Phys. Usp.*, **59**, 1129 (2016) [*Usp. Fiz. Nauk*, **186**, 1229 (2016)].
3. Anderson M.H., Ensher J.R., Matthews M.R., Wieman C.E., Cornell E.A. *Science*, **269**, 198 (1995).
4. Truscott A.G., Strecker K.E., McAlexander W.I., Partridge G.B., Hulet R.G. *Science*, **291**, 2570 (2001).
5. Ryabtsev I.I., Beterov I.I., Tretyakov D.B., Entin V.M., Yakshina E.A. *Phys. Usp.*, **59**, 196 (2016) [*Usp. Fiz. Nauk*, **186**, 206 (2016)].
6. Vishnyakova G.A., Golovizin A.A., Kalganova E.S., Sorokin V.N., Sukachev D.D., Tregubov D.O., Khabarova K.Yu., Kolachevsky N.N. *Phys. Usp.*, **59**, 168 (2016) [*Usp. Fiz. Nauk*, **186**, 176 (2016)].

7. Taichenaichev A.V., Yudin V.I., Bagayev S.N. *Phys. Usp*., **59**, 184 (2016) [*Usp. Fiz. Nauk*, **186**, 193 (2016)].
8. De Angelis M., Bertoldi A., Cacciapuoti L., Giorgini A., Lamporesi G., Prevedelli M., Saccorotti G., Sorrentino G., Tino G.M. *Measur. Sci. Technol.*, **20**, 022001 (2009).
9. Makhalov V.B., Martiyanov K.A., Turlapov A.V. *Metrologia*, **53**, 1287 (2016).
10. Jousten K. *Measurement*, **45**, 2420 (2012).
11. Calcatelli A. *Measurement*, **46**, 1029 (2013).
12. Redhead P.A.J. *Vac. Sci. Technol. A*, **2**, 132 (1984).
13. Watanabe F.J. *Vac. Sci. Technol. A*, **28**, 486 (2010).
14. Summers R. *NASA Technical Note TN D-5285* (Washington, DC: NASA, 1969).
15. Kendall B.R.F.J. *Vac. Sci. Technol. A*, **17**, 2041 (1999).
16. Peksa L., Prazak D., Gronych T., Repa P., Viear M., Tesar J., Krajıeek Z., Stanık F. *J. Metrology Soc. India*, **24**, 77 (2009).
17. Jousten K., Menzer H., Wandrey D., Niepraschk R. *Metrologia*, **36**, 493 (1999).
18. Raab E.L., Prentiss M., Cable A., Chu S., Pritchard D.E. *Phys. Rev. Lett.*, **59**, 2631 (1987).
19. Monroe C., Swann W., Robinson H., Wieman C. *Phys. Rev. Lett.*, **65**, 1571 (1990).
20. Takekoshi T., Knize R.J. *Opt. Lett.*, **21**, 77 (1996).
21. Grimm R., Weidemüller M., Ovchinnikov Y.B. *Optical Dipole Traps for Neutral Atoms* (New Uork: Acad. Press, 2000).
22. Booth J.L., Fagnan D.E., Klappauf B.G., Madison K.W., Wang J. Patent US 8803072 B2 (2014).
23. Arpornthip T., Sackett C.A., Hughes K.J. *Phys. Rev. A*, **85**, 033420 (2012).
24. O'Hara K.M., Granade S.R., Gehm M.E., Savard T.A., Bali S., Freed C., Thomas J.E. *Phys. Rev. Lett.*, **82**, 4204 (1999).
25. Dean K.R., Debeaux G., Wüest A., Garg R. *J. Photopolymer Sci. Technol.*, **20**, 393 (2007).
26. Herman M.A., Sitter H. *Molecular Beam Epitaxy: Fundamentals and Current Status* (Springer, 2012).
27. Bergeman T., Erez G., Metcalf H.J. *Phys. Rev. A*, **35**, 1535 (1987).
28. Prentiss M., Raab E.L., Pritchard D.E., Cable A., Bjorkholm J.E., Chu S. *Opt. Lett.*, **13**, 452 (1988).
29. Steane A.M., Chowdhury M., Foot C.J. *J. Opt. Soc. Am. B*, **9**, 2142 (1992).
30. Gensemer S.D., Sanchez-Villicana V., Tan K.Y.N., Grove T.T., Gould P.L. *Phys. Rev. A*, **56**, 4055 (1997).
31. Fagnan D.E., Wang J., Zhu C., Djuricanin P., Klappauf B.G., Booth J.L., Madison K.W. *Phys. Rev. A*, **80**, 022712 (2009).
32. Van Dongen J., Zhu C., Clement D., Dufour G., Booth J.L., Madison K.W. *Phys. Rev. A*, **84**, 022708 (2011).
33. Gerton J.M., Sackett C.A., Frew B.J., Hulet R.G. *Phys. Rev. A*, **59**, 1514 (1999).
34. Petrich W., Anderson M.H., Ensher J.R., Cornell E.A. *Phys. Rev. Lett.*, **74**, 3352 (1995).
35. Davis K.B., Mewes M.-O., Joffe M.A., Andrews M.R., Ketterle W. *Phys. Rev. Lett.*, **74**, 5202 (1995).
36. Cornell E.A., Ensher J.R., Wieman C.E. arXiv:cond-mat/9903109 (1999).
37. Savard T.A., O'Hara K.M., Thomas J.E. *Phys. Rev. A*, **56**, R1095 (1997).
38. Takekoshi T., Yeh J.R., Knize R.J. *Opt. Commun.*, **114**, 421 (1995).
39. Landau L.D., Lifshitz E.M. *Electrodynamics of Continuous Media* (Oxford: Pergamon Press 1960; Moscow: Fizmatlit, 2003).
40. Granade S.R., Gehm M.E., O'Hara K.M., Thomas J.E. *Phys. Rev. Lett.*, **88**, 120405 (2002).
41. Luo L., Clancy B., Joseph J., Kinast J., Turlapov A., Thomas J.E. *New J. Phys.*, **8**, 213 (2006).
42. Bali S., O'Hara K.M., Gehm M., Granade S.R., Thomas J.E. *Phys. Rev. A*, **60**, R29 (1999).
43. Landau L.D., Lifshitz E.M. *Quantum Mechanics (Nonrelativistic Theory)* (Oxford: Pergamon Press 1965; Moscow: Fizmatlit, 2002).
44. Dalgarno A. *Adv. Chem. Phys.*, **12**, 143 (1967).
45. Leck J.H. *Total and Partial Pressure Measurement in Vacuum Systems* (Springer, 1989).
46. Tilford C.R.J. *Vac. Sci. Technol. A*, **1**, 152 (1983).
47. Singleton J.H.J. *Vac. Sci. Technol. A*, **19**, 1712 (2001).
48. Julienne P.S., Smith A.M., Burnett K. *Theory of Collisions Between Laser Cooled Atoms* (New York: Acad. Press, 1992).
49. Houbiers M., Stoof H.T.C., McAlexander W.I., Hulet R.G. *Phys. Rev. A*, **57**, R1497 (1998).
50. Mart'yanov K.A., Makhalov V.B., Turlapov A.V. *JETP Lett*., **91**, 369 (2010) [*Pis'ma Zh. Eksp. Teor. Fiz.*, **91**, 401 (2010)].
51. Windholz L., Musso M., Zerza G., Jäger H. *Phys. Rev. A*, **46**, 5812 (1992).
52. Hong S.-S., Shin Y.-H., Arakawa I. *Meas. Sci. Technol.*, **15**, 359 (2004).
53. Bennett J.R.J., Hughes S., Elsey R.J., Parry T.P. *Vacuum*, **73**, 149 (2004).
54. Hong S.S., Shin Y., Kim J.T. *Measurement*, **41**, 1026 (2008).
55. Derevianko A., Johnson W.R., Safronova M.S., Babb J.F. *Phys. Rev. Lett.*, **82**, 3589 (1999).
56. Porsev S.G., Derevianko A. *Phys. Rev. A*, **65**, 020701 (2002).
57. Tkatchenko A., Scheffler M. *Phys. Rev. Lett.*, **102**, 073005 (2009).